Ezgi Yalçıntaş*, Xavier Gaona, Andreas C. Scheinost, Taishi Kobayashi, Marcus Altmaier, and Horst Geckeis

Redox chemistry of Tc(VII)/Tc(IV) in dilute to concentrated NaCl and $MgCl_2$ solutions

Abstract: The redox behaviour of Tc(VII)/Tc(IV) was investigated within the pH_c range 2–14.6 in (0.5 M and 5.0 M) NaCl and (0.25 M, 2.0 M and 4.5 M) $MgCl_2$ solutions in the presence of different reducing agents ($Na_2S_2O_4$, Sn(II), Fe(II)/Fe(III), Fe powder) and macroscopic amounts of Fe minerals (magnetite, mackinawite, siderite: S/L = 20–30 g L^{-1}). In the first group of samples, the decrease of the initial Tc concentration (1×10^{-5} M, as Tc(VII)) indicated the reduction to Tc(IV) according to the chemical reaction $TcO_4^- + 4H^+ + 3e^- \Leftrightarrow TcO_2 \cdot 1.6H_2O(s) + 0.4H_2O$. Redox speciation of Tc in the aqueous phase was further confirmed by solvent extraction. A good agreement is obtained between the experimentally determined Tc redox distribution and thermodynamic calculations based on NEA–TDB (Nuclear Energy Agency, Thermochemical Database) and ionic strength corrections by SIT or Pitzer approaches. These observations indicate that experimental pH_c and E_h values in buffered systems can be considered as reliable parameters to predict the redox behaviour of Tc in dilute to highly concentrated NaCl and $MgCl_2$ solutions. E_h of the system and aqueous concentration of Tc(IV) in equilibrium with $TcO_2 \cdot 1.6H_2O(s)$ are strongly affected by elevated ionic strength, especially in the case of 4.5 M $MgCl_2$ solutions. In such concentrated brines and under alkaline conditions ($pH_c = pH_{max} \sim 9$), kinetics play a relevant role and thermodynamic equilibrium for the system Tc(IV)(aq) ⇔ Tc(IV)(s) was not attained from oversaturation conditions within the timeframe of this study (395 days). Tc(VII) is reduced to Tc(IV) by magnetite, mackinawite and siderite suspensions at $pH_c = 8–9$ in concentrated NaCl and $MgCl_2$ solutions. Sorption is very high in all cases ($R_d \geq 10^3$ L kg^{-1}), although R_d values are significantly lower in 4.5 M $MgCl_2$ solutions. XANES (X-ray absorption near edge spectroscopy) evaluation of these samples confirms that Tc(VII) is reduced to Tc(IV) by Fe(II) minerals also in concentrated NaCl and $MgCl_2$ brines.

Keywords: Technetium, redox reactions, salt brines, thermodynamics, Fe(II) minerals, XANES.

DOI 10.1515/ract-2014-2272
Received April 1, 2014; accepted August 11, 2014

1 Introduction

^{99}Technetium is a β-emitting fission product primarily produced in nuclear reactors by the fission of ^{235}U and ^{239}Pu. Due to its high fission yield, long half-life ($t_{1/2} \sim 2.1 \times 10^5$ y) and redox-sensitive character, a reliable prediction of the chemical behaviour of technetium is necessary for the long-term safety assessment of nuclear waste repositories. In the case of repositories in salt-rock formations, the boundary conditions may potentially include saturated NaCl and $MgCl_2$ brines with salt concentrations above ~ 5 M and ~ 4.5 M, respectively. Technetium is also a relevant contaminant associated with sites for nuclear fuel reprocessing or plutonium production. Among the latter, the Hanford site (Washington State, USA) probably represents the largest remediation effort in the United States. In this site, Tc is mainly found as soluble species in the supernatant of underground storage tanks, which mostly consist of concentrated aqueous solutions of sodium nitrate/nitrite salts and sodium hydroxide [1, 2].

The chemical behaviour of radionuclides in concentrated salt brines can significantly differ from observations made in dilute solutions. Strong interaction processes between dissolved radionuclide species and the main background electrolyte ions can importantly modify the stability of charged species at elevated ionic strength. In some cases, the formation of new aquatic species and complexes unknown in dilute systems takes place in concentrated solutions, as recently reported for An(III/IV/V) in concentrated $CaCl_2$ brines [3–5]. Hence, the chemical behaviour

***Corresponding author: Ezgi Yalçıntaş,** Institute for Nuclear Waste Disposal, Karlsruhe Institute of Technology, Germany, e-mail: ezgi.yalcintas@kit.edu
Xavier Gaona, Marcus Altmaier, Horst Geckeis: Institute for Nuclear Waste Disposal, Karlsruhe Institute of Technology, Germany
Andreas C. Scheinost: Institute of Resource Ecology, Helmholtz-Zentrum Dresden-Rossendorf, Germany; and Rossendorf Beamline (ROBL) at ESRF, Grenoble, France
Taishi Kobayashi: Department of Nuclear Engineering, Kyoto University, Japan

and mobility of radionuclides under high ionic strength conditions cannot be simply extrapolated from dilute systems but need to be investigated for particular saline systems.

The mobility of Tc is strongly dependent on its oxidation state. Although several oxidation states of Tc are reported in the literature (ranging from +II to +VII) [6–9], Tc(VII) and Tc(IV) are the prevailing long-term stable redox states in the absence of any complexing ligand other than water under non reducing and reducing conditions, respectively. Heptavalent Tc exists as highly soluble and mobile pertechnetate anion (TcO_4^-), whereas Tc(IV) forms sparingly soluble hydrous oxides ($TcO_2 \cdot xH_2O(s)$). Due to the very different mobility and chemical characteristics of both oxidation states, an appropriate knowledge of the redox chemistry of Tc(VII)/Tc(IV) and Tc(IV) solubility/sorption processes is of special relevance in the context of radioactive waste disposal, as well as in the assessment of Tc behaviour in contaminated sites.

The redox transformations of Tc(VII)/Tc(IV) in the presence of different reducing systems were previously assessed in a number of experimental studies mostly in low ionic strength systems. Owunwanne *et al.* (1977) [10] and Warwick *et al.* (2007) [11] used Sn(II) to study the reduction of Tc(VII) under highly acidic (pH < 2) and hyperalkaline (pH > 13.3) conditions, respectively. A fast and complete reduction of Tc(VII) was observed in both cases. Hess *et al.* [12] obtained a well-defined $TcO_2 \cdot xH_2O$ solid phase by reducing Tc(VII) with $Na_2S_2O_4$. The resulting Tc(IV) solid phase was used in undersaturation solubility experiments under saline (≤ 5.0 M NaCl) and acidic (≤ 6.0 M HCl) conditions. Based on their solubility and spectroscopic (UV–VIS/NIR, EXAFS) data, the authors derived comprehensive thermodynamic and activity models for Tc(IV) valid up to $pH_c \sim 7$. Cui *et al.* (1996a) [13] reported a kinetically hindered reduction of Tc(VII) to Tc(IV) in the presence of aqueous Fe(II), whereas Fe(II) precipitated or sorbed on the vessel walls led to a rapid reduction of Tc(VII) at pH > 7.5. Zachara *et al.* (2007) [14] also studied the reduction of Tc(VII) in the presence of Fe(II)(aq) under near-neutral pH conditions ($6 \leq pH \leq 8$). In contrast to Cui and co-workers, the authors observed the reduction of Tc(VII) at pH ≥ 6.8, although reduction kinetics were strongly dependent on pH.

The role of Fe solid phases in the reduction of Tc(VII) has been intensively studied within the last decades. Among Fe phases, magnetite (Fe_3O_4) is often considered as one of the most relevant corrosion product of steel forming under the strongly reducing conditions expected in underground repositories for nuclear waste disposal. Cui *et al.* (1996b) [15] studied the uptake of Tc by magnetite in the presence of synthetic ground water. The authors assessed the effect of ionic strength and pH (7.8–9.5), investigated the rate of the sorption reaction, and concluded that the uptake was controlled by a ligand exchange mechanism. Geraedts *et al.* (2002) [16] and Maes *et al.* (2004) [17] studied the system magnetite–Tc in the presence of natural and synthetic Gorleben groundwater. The authors concluded that $TcO_2 \cdot xH_2O(s)$ formed in this system, and suggested that Tc(IV) polymers or colloids were responsible for the observed increase in solubility ($\sim 10^{-6}$ M). Wharton *et al.* (2000) [18] studied the coprecipitation of Tc(VII) and Tc(IV) with mackinawite (FeS) and characterized the resulting solid phases by X–ray absorption spectroscopy. Tc was immobilized as a $Tc^{IV}S_2$-like phase regardless of the initial oxidation state of Tc. Similar observations were reported by Livens *et al.* (2004) [19], who investigated the interaction between Tc and mackinawite using both +VII and +IV as initial redox state of Tc. Liu *et al.* (2008) [20] performed comprehensive immobilization experiments with Tc in the presence of mackinawite. The authors assessed the effect of ionic strength (≤ 1.0 M NaCl) and pH (6.1–9.0) on the uptake of Tc, and observed a strong pH–dependence and the increase of the uptake rate with increasing ionic strength. In contrast to Livens and co-workers, TcO_2-like instead of TcS_2-like phases were reported to form on the surface of mackinawite. Llorens *et al.* (2008) [21] coprecipitated Tc(VII) with siderite ($FeCO_3$), an Fe(II) solid phase forming in the presence of carbonate-rich groundwaters. The reduction of Tc(VII) and incorporation of Tc(IV) into the structure of siderite were confirmed by X–ray diffraction and transmission electron microscopy. Peretyazhko *et al.* (2012) [22] studied the reduction of Tc by reactive ferrous iron forming in naturally anoxic, redox transition zone sediments from the Hanford site. A number of Fe(II) minerals were identified in the sediments, including Fe(II)–phyllosilicates, pyrite, magnetite and siderite. The authors observed $TcO_2 \cdot xH_2O$-like phases regardless of Fe(II) mineralogy or reduction rate.

Recently, Kobayashi and co–workers [23] systematically assessed the reliability of E_h–pH measurements and reaction kinetics to explain the redox behaviour of Tc(VII)/Tc(IV) in dilute solutions (0.1 M NaCl) in the presence of homogeneous and heterogeneous reducing systems. The authors compared their experimental data with available thermodynamic predictions for Tc [24], and reported an experimental borderline for Tc(VII)/Tc(IV) reduction about 100 mV below the borderline calculated thermodynamically. This observation was explained by the formation of $TcO_2 \cdot xH_2O$(coll, hyd) colloidal particles with higher solubility than the solid

phase $TcO_2 \cdot 1.6H_2O(s)$ selected in the NEA–TDB review. In heterogeneous systems (presence of mineral phases), the reduction of Tc(VII) occurred only in the presence of magnetite, mackinawite and siderite phases.

In spite of the large number of experimental studies focussing on Tc redox reactions, the understanding of Tc(VII)/Tc(IV) redox processes and Tc(IV) uptake by Fe minerals is mostly limited to dilute aqueous systems, and investigations addressing Tc redox chemistry in concentrated salt brine systems remain very scarce. In this work, the redox behaviour of Tc(VII)/Tc(IV) couple was investigated in NaCl (0.5 M and 5.0 M) and $MgCl_2$ (0.25 M, 2.0 M and 4.5 M) solutions. The reduction of Tc(VII) to Tc(IV) was assessed in the presence of different reducing systems, *e.g.* $Na_2S_2O_4$, Sn(II), Fe(II)/Fe(III), Fe powder, magnetite, mackinawite and siderite. The results are systematised according to the experimental E_h and pH values of the solution/suspension, the measured Tc concentration and redox state and compared to thermodynamic calculations (using SIT (Specific Ion Interaction Theory) or Pitzer ion interaction models for ionic strength corrections). XANES was used to characterize the redox state of Tc sorbed by magnetite, mackinawite and siderite in concentrated brine solutions. Using a similar experimental and conceptual approach, the studies reported here extend the study published by Kobayashi *et al.* to other electrolyte systems and high ionic strength conditions.

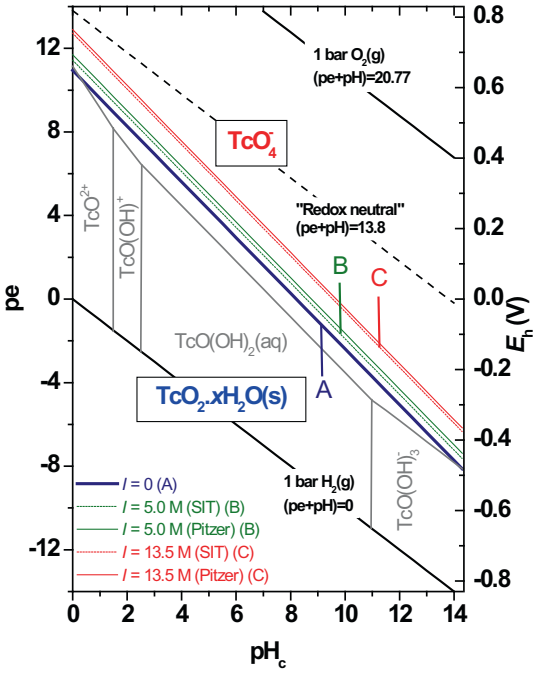

Fig. 1: *Pourbaix* diagram of Tc calculated for $I = 0$ with thermodynamic data selected in NEA–TDB [25]. Thin dark grey lines correspond to 50 : 50 distribution borderlines between aqueous Tc species at $I = 0$. Black lines indicate upper and lower decomposition lines of water and "redox neutral" (pe + pH = 13.8) conditions. Colored lines (A, B, C) correspond to Tc(VII)/Tc(IV) borderlines considering reaction (1), calculated for (A) $I = 0$ (blue line), (B) $I = 5.0$ M (green dashed line: SIT, green solid line: Pitzer; 5.0 M NaCl) and (C) $I = 13.5$ M (red dashed line: SIT, red solid line: Pitzer; 4.5 M $MgCl_2$). All calculations performed at $[Tc]_{tot} = 10^{-5}$ M. Ionic strength corrections performed by SIT and Pitzer approaches as described in Sects. 2.1 and 2.2.

2 Thermodynamic background

The thermochemical database project of the Nuclear Energy Agency (NEA–TDB) comprises the most comprehensive selection of thermodynamic data currently available for actinides and fission products. Technetium was initially reviewed in the volume 3 of the NEA–TDB series [25], although the thermodynamic selection was later revisited in the update volume by Guillaumont and co-authors [24]. The outcome is a critically reviewed selection of Tc thermodynamic data, rather complete for Tc(VII)/Tc(IV) redox reactions and Tc(IV) hydrolysis, solubility and carbonate complexation. The data selection is limited or non-existent for other potentially relevant ligands such as chloride, phosphate or sulphate. No ion interaction coefficients are selected for ionic species of Tc, thus limiting the applicability of the selected thermodynamic data to diluted systems where no specific ion interaction must be considered.

Figure 1 shows the *Pourbaix* diagram of Tc within $0 \le pH_c \le 14$ and $-14 \le pe \le 14$ as calculated with the current NEA–TDB data selection. Only Tc(VII) and Tc(IV) species appear in the diagram, although aqueous Tc(III) species (not currently selected in the NEA–TDB) have been reported to form under very acidic and reducing conditions [9, 26]. Due to the very low solubility of Tc(IV), one of the most relevant redox reactions of Tc corresponds to the reduction of TcO_4^- to the solid $TcO_2 \cdot 1.6H_2O(s)$ phase according to

$$TcO_4^- + 4H^+ + 3e^- \Leftrightarrow TcO_2 \cdot 1.6H_2O(s) + 0.4H_2O \quad \log {}^*K'_{VII-IVs} \qquad (1)$$

where $\log {}^*K'_{VII-IVs}$ is the conditional equilibrium constant for the reduction of TcO_4^- to $TcO_2 \cdot 1.6H_2O(s)$ at $I = 0$. The blue solid line (A) in Figure 1 corresponds to the thermodynamic borderline for Tc(VII)/Tc(IV) calculated at $I = 0$ according to reaction (1) and represents 50% Tc(VII) and 50% Tc(IV) redox state distribution. Note that this borderline depends both upon ionic strength and total Tc concentration, the later held constant at $[Tc]_0 = 1 \times 10^{-5}$ M in the calculations consistent with the exper-

imental conditions selected in this study (see Sect. 3.3). At $I \neq 0$, chemical equilibria are affected by ion interaction processes and activity coefficients need to be taken into account. Because of the high ionic strength in the experiments described in this work (up to $I = 5.0$ M in NaCl and $I = 13.5$ M in $MgCl_2$ systems), SIT and Pitzer approaches were used to calculate $\gamma_{TcO_4^-}$ and γ_{H^+} and thus determine $\log {}^*K'_{VII-IVs}$ for each ionic strength according with Eqs. (2)–(3).

$$\log {}^*K^\circ_{VII-IVs} = -\log\left([TcO_4^-]\cdot\gamma_{TcO_4^-}\right) - 4\log([H^+]\cdot\gamma_{H^+}) + 3pe + 0.4\log a_w \quad (2)$$

$$\log {}^*K'_{VII-IVs} = \log {}^*K^\circ_{VII-IVs} + \log\gamma_{TcO_4^-} + 4\log\gamma_{H^+} - 0.4\log a_w \quad (3)$$

Table 1 summarizes the values of $\log\gamma_{TcO_4^-}$, $\log\gamma_{H^+}$ and $\log {}^*K'_{VII-IVs}$ in NaCl (0.5 M and 5.0 M) and $MgCl_2$ (0.25 M, 2.0 M and 4.5 M) calculated by SIT and Pitzer models as described in Sects. 2.1 and 2.2, respectively. Tc(VII)/Tc(IV) redox borderlines calculated for NaCl and $MgCl_2$ solutions using $\log {}^*K'_{VII-IVs}$ are compared in the following sections with Tc redox distribution determined experimentally for each independent reducing system. Borderlines for Tc(VII)/Tc(IV) reduction calculated for 5.0 M NaCl and 4.5 M $MgCl_2$ are also included in Figure 1. The comparison of thermodynamic calculations for $I = 0$ (solid blue line (A)), $I = 5.0$ M (green lines (B), 5.0 M NaCl) and $I = 13.5$ M (red lines (C), 4.5 M $MgCl_2$) clearly indicates that a stabilization of Tc(IV) relative to Tc(VII) is expected with increasing ionic strength. Only minor differences (≤ 0.3 pe-units) are observed between Tc(VII)/Tc(IV) borderlines calculated by SIT and Pitzer, indicating the validity of the SIT also in the extremely high saline conditions of this study.

Table 1: Activity coefficients of TcO_4^- and H^+ in (0.5 and 5.0 M) NaCl and (0.25, 2.0 and 4.5 M) $MgCl_2$ solutions derived from SIT and Pitzer approaches (see Sects. 2.1 and 2.2). Conditional equilibrium constants ($\log^* K'_{VII-IVs}$) for reaction (1) are calculated for the corresponding ionic strengths conditions according to Eq. (3).

Background electrolyte	$\log\gamma_{H^+}$		$\log\gamma_{TcO_4^-}$		$\log {}^*K'_{VII-IVs}$	
	SIT	Pitzer	SIT	Pitzer	SIT	Pitzer
0.5 M NaCl	−0.11	−0.10	−0.17	−0.19	37.2	37.2
5.0 M NaCl	0.41	0.59	−0.21	−0.16	39.3	40.1
0.25 M $MgCl_2$	−0.13	−0.19	−0.11	−0.06	37.2	37.0
2.0 M $MgCl_2$	0.24	0.21	0.43	0.50	39.2	39.2
4.5 M $MgCl_2$	0.95	1.06	1.41	1.51	43.2	43.7

2.1 Thermodynamic SIT model

The specific ion interaction theory (SIT approach [27]) is the method adopted by NEA–TDB [24] for the treatment of ion interaction processes and ionic strength effects. The validity of SIT is normally limited to $I_m \leq 3.0$ M [28], although recent publications have shown a good performance of SIT far beyond this limit in concentrated $MgCl_2$ and $CaCl_2$ solutions [4, 5]. Activity coefficients in SIT are calculated according to Eq. (4):

$$\log\gamma_j = -z_j^2 D + \sum_k \varepsilon(j,k) m_k \quad (4)$$

where z_j is the charge of ion j, D is the Debye–Hückel term, m_k is molality of the oppositely charged ion k and $\varepsilon(j,k)$ is the specific ion interaction parameter. Thus, the ionic strength dependence of $\log {}^*K'_{VII-IVs}$ in NaCl and $MgCl_2$ solutions can be calculated by SIT based on equations (5) and (6), respectively:

$$\log {}^*K'_{VII-IVs} = \log {}^*K^\circ_{VII-IVs} - 0.4\log a_w - 5D + \varepsilon\left(TcO_4^-, Na^+\right) m_{Na^+} + 4\varepsilon\left(H^+, Cl^-\right) m_{Cl^-} \quad (5)$$

$$\log {}^*K'_{VII-IVs} = \log {}^*K^\circ_{VII-IVs} - 0.4\log a_w - 5D + \varepsilon\left(TcO_4^-, Mg^{2+}\right) m_{Mg^{2+}} + 4\varepsilon\left(H^+, Cl^-\right) m_{Cl^-} \quad (6)$$

No SIT ion interaction coefficients are selected for TcO_4^- in the NEA–TDB. The chemical analogy of TcO_4^- with ClO_4^- is therefore considered in this work to estimate the corresponding SIT coefficients with Na^+ and Mg^{2+}, yielding $\varepsilon(TcO_4^-, Na^+) \cong \varepsilon(ClO_4^-, Na^+) = 0.01 \pm 0.01$ kg mol^{-1} and $\varepsilon(TcO_4^-, Mg^{2+}) \cong \varepsilon(ClO_4^-, Mg^{2+}) = 0.33 \pm 0.03$ kg mol^{-1} [24]. The activity of water in dilute to concentrated NaCl and $MgCl_2$ solutions, as well as $\varepsilon(H^+, Cl^-) = 0.12 \pm 0.01$ kg mol^{-1} were taken directly from the NEA–TDB [24].

2.2 Thermodynamic Pitzer model

Due to the known limitations of the SIT approach at high ionic strengths, the use of the Pitzer formulism is strongly recommended for thermodynamic calculations and geochemical modelling in concentrated salt brine solutions [29]. The Pitzer approach describes the interactions between a cation c and an anion a by the binary parameters $\beta^{(0)}_{ca}$, $\beta^{(1)}_{ca}$ and $C^{(\varphi)}_{ca}$ and mixing parameters $\theta_{cc'}$ (or $\theta_{aa'}$) and $\Psi_{c'a}$(or $\Psi_{aa'c}$). The latter account for interactions with further cations c (or anions a) in ternary or higher multicomponent electrolyte solutions. The values of $\log\gamma_{H^+}$ and a_w in equation (2) used in this study are calculated from the parameters reported by Harvie *et al.* [30]. Binary

Table 2: Pitzer ion interaction coefficients for TcO_4^- in NaCl and $MgCl_2$ media at 25 °C: $\beta_{ca}^{(0)}$, $\beta_{ca}^{(1)}$ and $\theta_{aa'}$ in [kg mol^{-1}]; $C_{ca}^{(\phi)}$ and $\Psi_{aa'c}$ in [kg^2 mol^{-2}].

		Binary Pitzer parameters			Ternary Pitzer parameters			
a	c	$\beta_{ca}^{(0)}$	$\beta_{ca}^{(1)}$	$C_{ca}^{(\phi)}$	a'	$\theta_{aa'}$	$\Psi_{aa'c}$	Ref.
TcO_4^-	Na^+	0.01111	0.1595	0.00236	Cl^-	0.067	−0.0085	[31]
TcO_4^-	Mg^{2+}	0.3138	1.84	0.0114	Cl^-	0.067	−0.0115	[32]

parameters for (TcO_4^-, Na^+) and (TcO_4^-, Mg^{2+}), mixing parameter for (TcO_4^-, Cl^-) and ternary parameters for (TcO_4^-, Cl^-, Na^+) and (TcO_4^-, Cl^-, Mg^{2+}) were taken from Könnecke *et al.* [31] and Neck *et al.* [32] as summarized in Table 2.

3 Experimental

3.1 Chemicals

All solutions were prepared with purified water (Milli-Q academic, Millipore) and purged with Ar before use to remove traces of oxygen. All sample preparation and handling was performed in an Ar-glovebox at 22 ± 2 °C. A purified and radiochemically well-characterized ^{99}Tc stock solution (1.3 M $NaTcO_4$) was used for the experiments. NaCl (p.a.), $MgCl_2 \cdot 6H_2O$ (p.a.), $Mg(OH)_2$(cr), Na_2S, hydroquinone ($C_6H_4(OH)_2$), $Na_2S_2O_4$, and metallic iron powder (grain size 10 μm) were obtained from Merck; $FeCl_3 \cdot 6H_2O$, $SnCl_2$, $Fe(NH_4)_2(SO_4)_2 \cdot 6H_2O$, pH buffers MES (pH 5–7) and PIPES (pH 7–9), NH_4OH and tetraphenylphosphonium chloride (TPPC) were obtained from Sigma-Aldrich, and $FeCl_2$ from Alfa Aesar. HCl and NaOH Titrisol® (Merck) were used for adjusting the pH of solutions. Magnetite (Fe_3O_4), mackinawite (FeS) and siderite ($FeCO_3$) were synthesized following the protocol described elsewhere [33]. Magnetite and mackinawite were characterized by high energy powder XRD (D8 ADVANCE, Bruker). No XRD characterization was performed for siderite due to the rapid oxidation of the dry powder during measurement. However, the characteristic light-gray colour of siderite was retained in the aqueous samples throughout the equilibration time and subsequent XANES sample preparation performed in the glovebox.

3.2 pH and E_h measurements

The hydrogen ion concentration ($pH_c = -\log[H^+]$) was measured using combination pH electrodes (type ROSS, Orion) calibrated against standard pH buffers (pH 1–12, Merck). The values of $pH_c = pH_{exp} + A_c$ were calculated from the operational "measured" pH_{exp} using empirical corrections factors (A_c), which entail both the liquid junction potential and the activity coefficient of H^+. A_c values determined as a function of NaCl and $MgCl_2$ concentration are reported in the literature [34]. In NaCl–NaOH solutions with $[OH^-] > 0.03$ M, the H^+ concentration was calculated from the given fixed hydroxide concentration $[OH^-]$ and the conditional ion product K'_w of water. In $MgCl_2$ solutions, the highest pH is fixed by the precipitation of $Mg(OH)_2$(cr) (or $Mg_2(OH)_3Cl \cdot 4H_2O$(cr) in $MgCl_2 \geq 2$ m) which buffers pH conditions at $pH_c = pH_{max} \sim 9$ [34].

Redox potentials were measured with Pt combination electrodes with Ag/AgCl reference system (Metrohm) and converted to E_h *vs.* the standard hydrogen electrode by correction for the potential of the Ag/AgCl reference electrode (+208 mV for 3 M KCl at 25 °C). Stable E_h readings were obtained within 10 min in most of the samples, although in some cases longer equilibration times (up to 30′) were required. The apparent electron activity ($pe = -\log a_{e^-}$) was calculated from $E_h = -(RT/F)\ln a_{e^-}$, according to the relation $pe = 16.9\, E_h$ (V). The performance of the redox electrode was tested with a standard redox buffer solution (Schott, +220 mV *vs.* Ag/AgCl), which provided readings within ±10 mV of the certified value. Previous studies [35, 36] have suggested the need of (experimentally determined) correction factors for E_h measured at high ionic strengths, which should mostly account for variations in the liquid junction potential. Liquid junction potentials below 50 mV are expected in the conditions of this study [37]. These values are well within the uncertainty considered for E_h measurements, and thus the use of such corrections was disregarded in the present work.

3.3 Sample preparation and characterization

Batch experiments were performed in NaCl (0.5 M and 5.0 M) and $MgCl_2$ (0.25 M, 2.0 M and 4.5 M) in the

presence of different reducing systems (1 mM $Na_2S_2O_4$, 1 mM $SnCl_2$, 1 mM/0.1 mM Fe(II)/Fe(III), 1 mg/15 mL Fe powder). In some of these systems, the formation of a solid phase occurred at near-neutral to alkaline pH conditions ($SnCl_2$, Fe(II)/Fe(III) and Fe powder). In each experimental series, pH values were adjusted with either HCl–NaCl–NaOH or HCl–$MgCl_2$–$Mg(OH)_2$ of identical ionic strength. The initial Tc(VII) concentration was set to 1×10^{-5} M by addition of $NaTcO_4$ stock solution to the pre-equilibrated system.

Tc concentration in solution was monitored at regular time intervals (up to 395 days) by Liquid Scintillation Counting (LSC, Quantulus, Perkin Elmer) after 10 kD ultrafiltration (2–3 nm, Pall Life Sciences). Samples for LSC analysis were mixed with 10 mL of LSC–cocktail (Ultima Gold XR, Perkin–Elmer), resulting in a detection limit of ~ 10^{-9} M. Although several measurements were performed for each independent batch sample throughout the timeframe of the experiment, note that Figs. 2–5 show only equilibrium values (except indicated otherwise). The oxidation state of Tc in the aqueous phase was determined by solvent extraction as reported elsewhere [38, 39]. Briefly, the supernatant of the sample was contacted with an anion exchanger 50 mM tetraphenylphosphonium chloride (TPPC) in chloroform. After vigorous mixing for 1 minute and subsequent separation of the aqueous and organic phases by centrifugation, Tc concentration in the aqueous phase was determined by LSC and attributed to presence of Tc(IV).

Six additional samples in 5.0 M NaCl and 4.5 M $MgCl_2$ were prepared in the presence of macroscopic amounts of magnetite (solid-to-liquid ratio, S : L = 21 g L^{-1}), mackinawite (S : L = 30 g L^{-1}) and siderite (S : L = 20 g L^{-1}). Initial concentration of Tc(VII) was set to 2×10^{-4} M to allow XANES analysis, and a contact time of 4 weeks was adopted in all cases. pH_c, E_h and [Tc] (after 10 kD ultrafiltration) were determined before phase separation using centrifugation at 4020 *g*. The wet paste resulting after phase separation was placed into double confined sample holders, heat-sealed inside the Ar-glovebox and stored in a N_2 Dewar (Voyager 12, Air Liquide – DMC, France) until the collection of XANES spectra. This method has been previously proven to avoid changes in oxidation state of redox sensitive samples (*e.g.* Np, Pu and Tc) [23, 33, 40].

3.4 XANES measurements

X-ray absorption near-edge structure (XANES) spectra were acquired in fluorescence mode at the Tc *K*-edge (21 044 eV) at the Rossendorf Beamline (ROBLII), ESRF, Grenoble, France. The energy of the Si(111) double-crystal monochromator was calibrated using a Mo foil (edge energy 20 000 eV). Two Rh-coated mirrors were used to collimate the beam into the monochromator crystal and to reject higher-order harmonics. Fluorescence spectra were collected using a 13-element, high-purity, solid-state Ge detector (Canberra) with digital spectrometer (XIA XMAP). During the measurement, the samples were kept at 15 K with a closed-cycle He cryostat to avoid changes of oxidation state and to reduce thermal disorder in the samples [33]. The XANES spectra were compared with a reference spectra of TcO_4^- [41].

4 Results and discussion

4.1 Tc redox chemistry in reducing aqueous systems

Experimental E_h and pH_c values measured in NaCl and $MgCl_2$ solutions in the presence of reducing chemicals are summarized in the E_h–pH diagrams in Figs. 2–5. Colored dashed and solid lines in the figures represent the thermodynamic equilibrium between Tc(VII) and Tc(IV) (50 : 50 distribution borderline) calculated for reaction (1) by SIT and Pitzer approaches, respectively. These calculations were performed assuming a content of 1.6 H_2O molecules in the hydration sphere of $TcO_2 \cdot xH_2O$(s) according to literature [42]. The samples were regularly monitored for pH_c, E_h and [Tc] for up to 395 d. In order to clarify the graphs, only average values are plotted for samples where stable readings indicate that equilibrium has been reached. Tc concentration as a function of pH_c for each reducing system is provided besides the corresponding E_h–pH diagrams. Uncertainty associated to [Tc] is lower than 0.1 log-units. Only for a limited number of systems, kinetic processes are specifically addressed. The decrease of the Tc concentration in the aqueous phase is interpreted as the reduction of Tc(VII) and consequent formation of the $TcO_2 \cdot 1.6H_2O$(s) phase, which is sparingly soluble under the adopted conditions. Table 3 summarizes the redox distribution of Tc in the aqueous phase of selected samples as quantified by solvent extraction.

4.1.1 $Na_2S_2O_4$ systems

E_h–pH diagrams of Tc in 1 mM $Na_2S_2O_4$ are shown in Figure 2a (NaCl) and 2c ($MgCl_2$). In all samples, measured

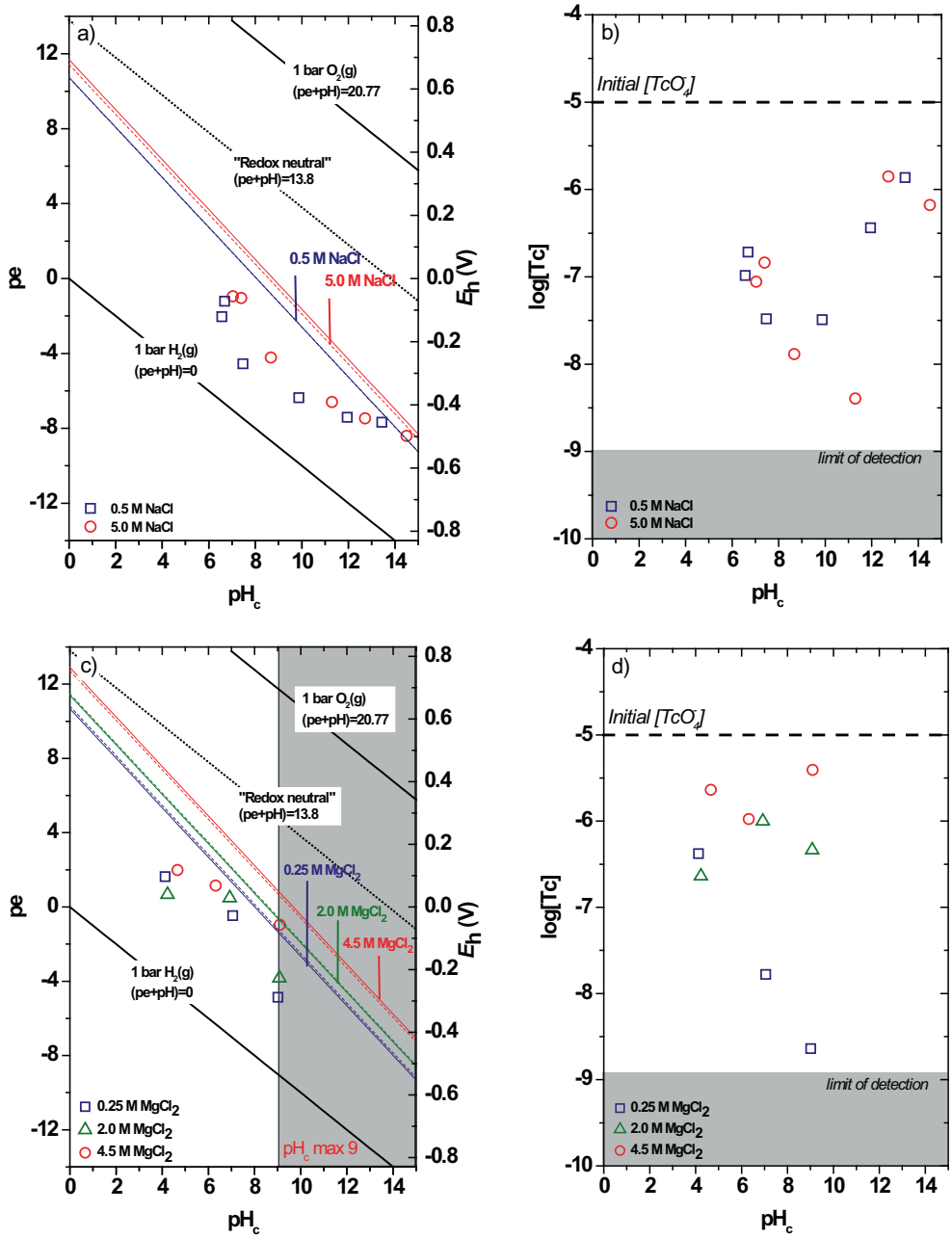

Fig. 2: Tc(VII)/Tc(IV) redox behaviour in the presence of 1 mM $Na_2S_2O_4$. NaCl solutions: (a) E_h–pH diagram, (b) aqueous concentration of Tc in NaCl solutions. $MgCl_2$ solutions: (c) E_h–pH diagram, (d) aqueous concentration of Tc in $MgCl_2$ solutions. Dashed and solid lines corresponding to the Tc(VII)/Tc(IV) redox borderline calculated for reaction (1) using NEA–TDB with SIT and Pitzer ionic strength corrections, respectively.

E_h values are below the thermodynamically expected Tc(VII)/Tc(IV) borderline. E_h values with large uncertainties (up to ±100 mV) are observed in near-neutral to slightly alkaline pH conditions. This observation is likely related with the known degradation of $Na_2S_2O_4$ under less alkaline to acidic pH conditions [43, 44]. No significant differences were observed between the E_h values measured in dilute and concentrated NaCl solutions. On the contrary, large differences (up to 5 pe-units) arise between E_h values measured in dilute and concentrated $MgCl_2$ solutions, hence hinting towards a strong impact of ionic strength, $[Cl^-]$ and/or $[Mg^{2+}]$ on the redox couple controlling the E_h in this system.

A significant decrease of Tc concentration indicating the reduction of Tc(VII) to Tc(IV) is observed in all systems with $Na_2S_2O_4$ (Figs. 2b and 2d). The predominance

Table 3: Tc redox distribution in the aqueous phase of selected samples in NaCl and $MgCl_2$ solutions, as quantified by solvent extraction after 10 kD ultrafiltration.

Reducing system	Background electrolyte	pH_c [a]	E_h (mV) [b]	%Tc(IV) [c]
$Na_2S_2O_4$	0.5 M NaCl	7.5	−270	98
$Na_2S_2O_4$	0.5 M NaCl	6.6	−120	99
$Na_2S_2O_4$	0.5 M NaCl	12.0	−435	92
$Na_2S_2O_4$	5.0 M NaCl	12.7	−445	99
Sn(II)	0.5 M NaCl	1.9	30	98
Sn(II)	0.5 M NaCl	13.7	−760	99
Sn(II)	5.0 M NaCl	2.9	80	92
Sn(II)	5.0 M NaCl	14.5	−760	99
Fe(II)/Fe(III)	0.5 M NaCl	2.0	645	0.4
Fe(II)/Fe(III)	5.0 M NaCl	2.8	400	0.1
Fe(II)/Fe(III)	5.0 M NaCl	4.5	635	0.4
$Na_2S_2O_4$	2.0 M $MgCl_2$	7.0	30	99
$Na_2S_2O_4$	4.5 M $MgCl_2$	9.0	−55	99
Sn(II)	2.0 M $MgCl_2$	3.7	5	73
Sn(II)	4.5 M $MgCl_2$	4.0	140	62
Sn(II)	4.5 M $MgCl_2$	6.4	−10	85
Sn(II)	4.5 M $MgCl_2$	9.0	−215	99
Fe(II)/Fe(III)	0.25 M $MgCl_2$	3.4	205	0.1
Fe(II)/Fe(III)	2.0 M $MgCl_2$	3.8	485	0.2
Fe(II)/Fe(III)	4.5 M $MgCl_2$	4.2	610	0.3
Fe(II)/Fe(III)	4.5 M $MgCl_2$	6.4	365	0.6
Fe powder	4.5 M $MgCl_2$	9.0	−195	99
Fe powder	4.5 M $MgCl_2$	8.9	−125	99

a: ±0.05; b: ±50 mV; c: ±10%.

of Tc(IV) in the aqueous phase is confirmed for selected samples by solvent extraction (Table 3). This is in very good agreement with thermodynamic calculations performed using NEA–TDB and SIT/Pitzer ionic strength corrections as summarized in Table 1. Higher concentrations of Tc(IV) are retained in the aqueous phase in NaCl solutions at $pH_c > 12$. This is consistent with the expected formation of an anionic hydrolysis species (*e.g.* $TcO(OH)_3^-$), which increases the solubility of $TcO_2 \cdot 1.6H_2O(s)$ in the strongly alkaline pH region. Similar to previous observations by Kobayashi and co-workers in diluted NaCl solutions and $Na_2S_2O_4$ [23], $\sim 10^{-7}$ M Tc(IV) concentrations are observed in 0.5 M and 5.0 M NaCl solutions under near-neutral pH conditions. A concentration level of 10^{-8}–10^{-9} M is expected for Tc(IV) solubility under these conditions according to the equilibrium reaction $TcO_2 \cdot 1.6H_2O(s) \Leftrightarrow TcO(OH)_2(aq) + 0.6H_2O$ [24]. This observation is also in disagreement with data obtained in the present work in Sn(II) systems (see Figure 3b), thus hinting towards a possible impact of $Na_2S_2O_4$ degradation on the behaviour of Tc(IV). Note that the formation of very stable colloidal Tc–S species has been previously reported in the literature [45].

Very high [Tc(IV)] (up to $10^{-5.5}$ M) is retained in solution in concentrated $MgCl_2$ systems, even in the slightly alkaline pH conditions buffered by the presence of $Mg(OH)_2$(cr) or $Mg_2(OH)_3Cl \cdot 4H_2O$(cr). The comparison of these results with Sn(II) and Fe(II)/Fe(III) systems suggests that [Tc(IV)] in equilibrium with $TcO_2 \cdot 1.6H_2O(s)$ in the presence of $Na_2S_2O_4$ can be overestimated, especially at near-neutral conditions.

4.1.2 Sn(II) systems

Tin(II) is a very strong reducing agent which keeps stable E_h values slightly above the border of water reduction (Figs. 3a and 3c). The redox couple Sn(II)/Sn(IV) controlling the E_h in this system is strongly impacted by ionic strength, $[Cl^-]$ and/or $[Mg^{2+}]$, with $pe + pH_c$ values ranging from 2 ± 1 to 7 ± 1 in 0.5 M NaCl and 4.5 M $MgCl_2$, respectively. Very similar $pe + pH_c$ values like in 0.5 M NaCl were recently reported for Sn(II) solutions in 0.1 M NaCl ($pe + pH_c = 2 \pm 1$) [23]. The very reducing E_h values fixed by Sn(II) promote a fast ($t_{1/2} = 7$ d) and complete reduction of Tc(VII) to Tc(IV) in NaCl solutions (Figure 3b). This observation is confirmed by solvent extraction, which indicates the predominance of Tc(IV) (≥ 92%) in all NaCl samples analysed (Table 3). The shape of the Tc(IV) solubility curve obtained from oversaturation in these systems is in excellent agreement with thermodynamic calculations performed at $I = 0$ according with NEA–TDB data selection (solid line in Figure 3b). This observation strongly suggests that equilibrium conditions have been attained in the system, as well as hinting towards the expected predominance of $TcO_2 \cdot 1.6H_2O(s)$ and TcO^{2+}, $TcO(OH)^+$, $TcO(OH)_2(aq)$ and $TcO(OH)_3^-$ as solubility controlling solid phase and Tc(IV) hydrolysis species in equilibrium, respectively. Tc concentrations determined in the acidic pH range are also in very good agreement with the undersaturation solubility data reported by Hess and co-workers [12] (also shown in Figure 3b). This indicates that the same solid phase has been obtained from oversaturation (present work) and undersaturation [12] conditions. Our data also confirm the strong effect of ionic strength on Tc(IV) solubility under acidic conditions, where [Tc] in equilibrium with $TcO_2 \cdot 1.6H_2O(s)$ increases 1.5–2 log-units between 0.5 M and 5.0 M NaCl. Note that in the pH-range of our study ($pH_c \geq 2$), the thermodynamic model by Hess and co-workers explains the increase of solubility by ion interaction phenomena, and disregards the formation of Tc(IV)–Cl complexes.

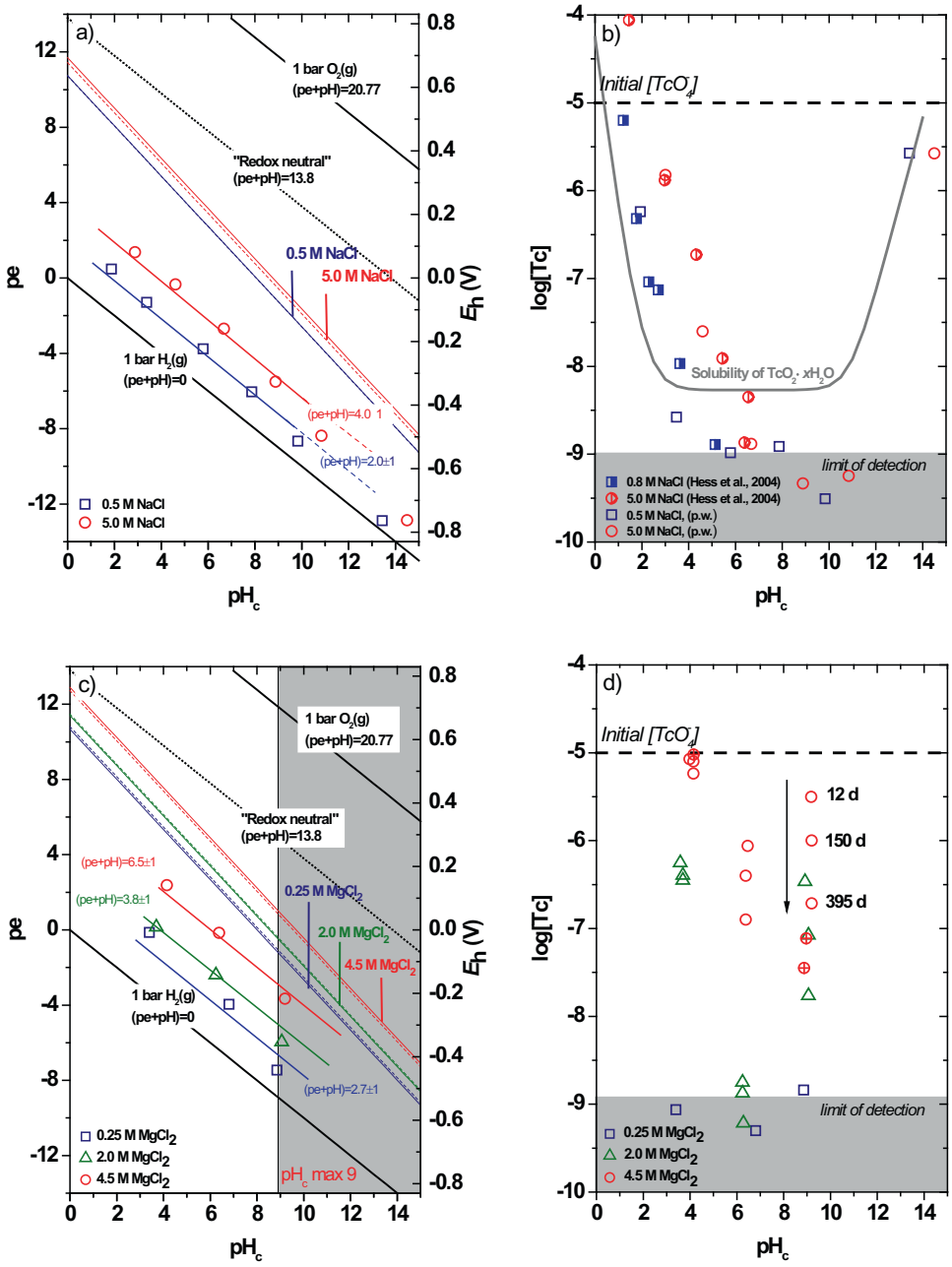

Fig. 3: Tc(VII)/Tc(IV) redox behaviour in the presence of 1 mM Sn(II). NaCl solutions: (a) E_h–pH diagram, (b) aqueous concentration of Tc in NaCl solutions. $MgCl_2$ solutions: (c) E_h–pH diagram, (d) aqueous concentration of Tc in $MgCl_2$ solutions. Dashed and solid lines corresponding to the Tc(VII)/Tc(IV) redox borderline calculated for reaction (1) using NEA–TDB with SIT and Pitzer ionic strength corrections, respectively. Solid grey line in (b) represents the solubility curve of $TcO_2 \cdot 1.6H_2O$(s) calculated at $I = 0$ using NEA–TDB. Symbol ⊕ in (d) indicates [Tc(IV)] in 4.5 M $MgCl_2$ measured from undersaturation conditions (see text).

Very low [Tc] are observed in 0.25 M $MgCl_2$ at $3.5 \leq pH_c \leq 9$ (Figure 3d), in good agreement with data in 0.5 M NaCl. Significantly higher [Tc] are observed in 2.0 M and 4.5 M $MgCl_2$. Both systems are affected by strong kinetics (especially for $pH_c = pH_{max} \sim 9$), which likely hinders thermodynamic equilibrium even after 395 d. This hypothesis was further evaluated by Tc(IV) solubility samples prepared from undersaturation. Within this approach, the solubility experiment is started with a macroscopic amount of solid phase contacted with Tc-free supernatant solution. A faster attainment of thermodynamic equilibrium is expected under these conditions, compared to the oversaturation approach where precipitation of rather ill-defined microcrystalline phases may oc-

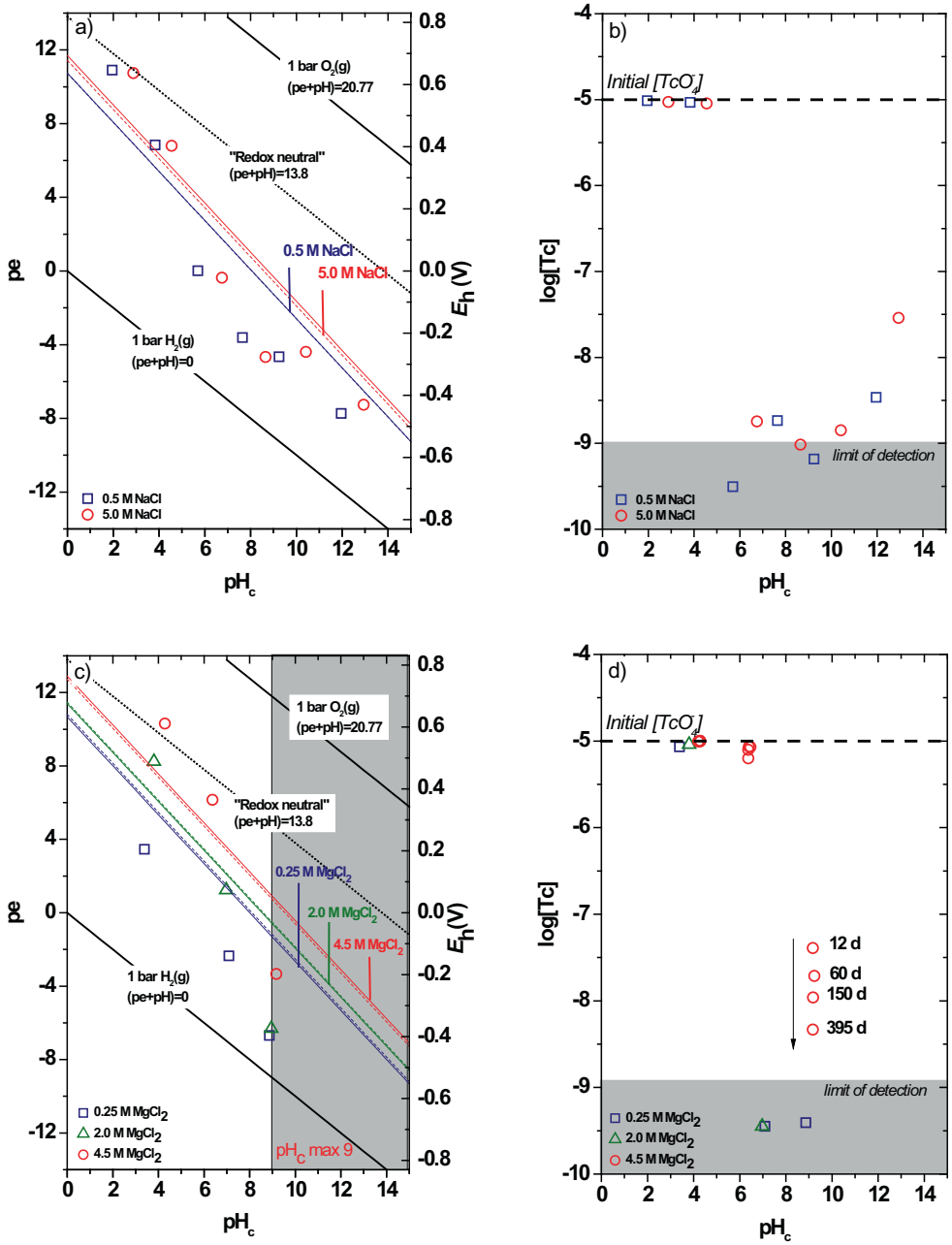

Fig. 4: Tc(VII)/Tc(IV) redox behaviour in the presence of Fe(II)/Fe(III). NaCl solutions: (a) E_h–pH diagram, (b) aqueous concentration of Tc in NaCl solutions. $MgCl_2$ solutions: (c) E_h–pH diagram, (d) aqueous concentration of Tc in $MgCl_2$ solutions. Dashed and solid lines corresponding to the Tc(VII)/Tc(IV) redox borderline calculated for reaction (1) using NEA–TDB with SIT and Pitzer ionic strength corrections, respectively.

cur. Hence, Tc(IV) prepared electrochemically was precipitated as $TcO_2 \cdot 1.6H_2O(s)$ [46] in a dilute NaOH solution ($pH_c \sim 11$), separated from the supernatant and contacted with two 4.5 M $MgCl_2$ solutions ($pH_c = 4$ and pH_{max}) in the presence of 2 mM Sn(II). The aqueous concentration of Tc(IV) in equilibrium with $TcO_2 \cdot 1.6H_2O(s)$ as determined from undersaturation conditions is marked as ⊕ in Figure 3. Lower Tc concentrations observed at pH_{max} in 4.5 M $MgCl_2$ support the trend observed from oversaturation and confirm that no thermodynamic equilibrium is attained after 395 d in these conditions. On the contrary, very similar [Tc] are measured at $pH_c = 4$ from undersaturation and oversaturation approaches, thus indicating that the same solid phase (expectedly $TcO_2 \cdot 1.6H_2O(s)$) is controlling the solubility in both cases and confirming

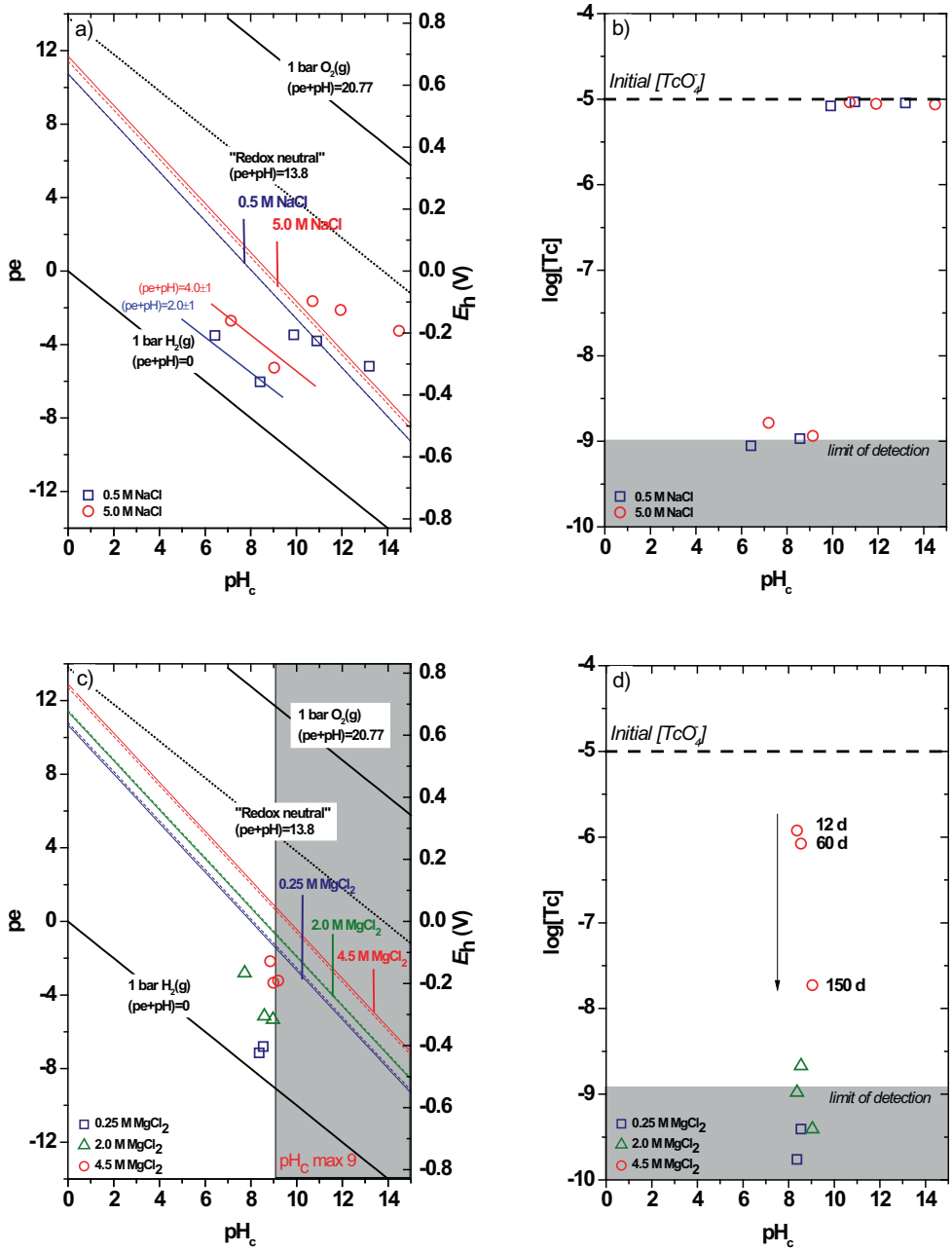

Fig. 5: Tc(VII)/Tc(IV) redox behaviour in the presence of Fe powder. NaCl solutions: (a) E_h–pH diagram, (b) aqueous concentration of Tc in NaCl solutions. $MgCl_2$ solutions: (c) E_h–pH diagram, (d) aqueous concentration of Tc in $MgCl_2$ solutions. Dashed and solid lines corresponding to the Tc(VII)/Tc(IV) redox borderline calculated for reaction (1) using NEA–TDB with SIT and Pitzer ionic strength corrections, respectively.

that thermodynamic equilibrium has been also attained in the latter case.

Solvent extraction analysis of the supernatant solution in 2.0 M and 4.5 M $MgCl_2$ indicates 62%–99% content in Tc(IV), depending upon pH and ionic strength (Table 3). Similar observations in concentrated NaCl solutions were reported by Hess and co-workers, who confirmed the predominance of Tc(IV) in the same samples using UV–VIS/NIR. Note that the solvent extraction method used in this work has been reported to extract into the organic phase not only MO_4^- species (M = Re, Mn, Tc, I) but also anionic chloride complexes such as $SnCl_6^{2-}$ and $ZnCl_4^{2-}$ [47]. Thus, the hypothetical formation of anionic Tc(IV)–Cl and/or Tc(IV)–OH–Cl species forming in concentrated Cl-brines may lead to an underestimation of Tc(IV) concentration in the aqueous phase. Dedicated

undersaturation solubility studies with Tc(IV) in dilute to concentrated NaCl, $MgCl_2$ and $CaCl_2$ are underway to assess these uncertainties and derive complete chemical, thermodynamic and activity models valid also in concentrated brines.

4.1.3 Fe(II)/Fe(III) systems

Figure 4 shows the redox behaviour of Tc(VII)/Tc(IV) in the presence of Fe(II)/Fe(III) in dilute to concentrated NaCl and $MgCl_2$ solutions. In analogy to $Na_2S_2O_4$ systems, the increase of ionic strength induces only a minor effect on the E_h values measured in NaCl solutions. For this background electrolyte system, the Fe(II)/Fe(III) redox pair define E_h values above the calculated Tc(VII)/Tc(IV) borderline under acidic pH conditions. At $pH_c = 2–3$, most of the initial $Fe(II)_{aq}$ and $Fe(III)_{aq}$ are retained in solution. For these conditions, E_h values can be thermodynamically calculated considering the chemical reaction $Fe^{2+} \Leftrightarrow Fe^{3+} + e^-$. Assuming $[Fe(II)]_0 = [Fe(II)]_{aq}$ and $[Fe(III)]_0 = [Fe(III)]_{aq}$, and considering $[Fe(II)]_{aq} = [Fe^{2+}]$ and $[Fe(III)]_{aq} = [Fe^{3+}] + \Sigma[FeCl_n^{3-n}] + \Sigma[Fe(OH)_n^{3-n}]$ at $pH_c = 2$ in 0.5 M NaCl, an E_h^{therm} value of 0.63 V can be calculated based on Eq. (7) and using $\log {}^*K^\circ$ and SIT ion interaction parameters summarized in Tables A1 and A2 in the Appendix.

$$\begin{aligned} pe = {} & \log(Fe(III)_{tot} \cdot \gamma_{Fe^{3+}}) - \log(Fe(II)_{tot} \cdot \gamma_{Fe^{2+}}) \\ & - \log K^\circ_{Fe^{2+}Fe^{3+}} - \log\left(1 + \sum {}^*\beta_{1,n,m} \cdot [Cl^-]^n \cdot [H^+]^{-m}\right) \end{aligned} \quad (7)$$

where ${}^*\beta_{1,n,m}$ are the conditional equilibrium constants for the formation of Fe(III) hydroxo and chloro complexes under given pH_c and $[Cl^-]$ conditions. This value is in excellent agreement with the measured redox potential (0.64 ± 0.05 V), thus supporting the validity of the E_h values experimentally determined in the Fe systems. E_h values below the calculated Tc(VII)/Tc(IV) borderline are measured in the near-neutral and alkaline pH regions. Under these conditions, the formation of a black Fe precipitate (likely magnetite) occurs. Thermodynamic calculations considering the formation of this solid phase predict the decrease of E_h towards more reducing conditions, although the exact redox potential is strongly dependent on the particle size of the solid forming (and thus on the selected $\log {}^*K^\circ_{s,0}$).

A clear decrease of Tc concentration occurs under near-neutral to hyperalkaline pH conditions indicating the reduction of Tc(VII), whereas [Tc] remains $\sim 10^{-5}$ M in the acidic pH region (Figure 4b). This is in good agreement with the thermodynamic borderline for 50:50% Tc(VII)/Tc(IV) redox distribution calculated with NEA–TDB and SIT/Pitzer ionic strength corrections as described in Sect. 2. These observations are also in line with data reported by Zachara and co-workers, who observed a rapid reduction of Tc(VII) in the presence of Fe(II) at pH > 6.8 [14]. In contrast to this, Cui *et al.* [13] reported the absence of Tc(VII) reduction in Fe(II) systems with $pH \leq 7.5$.

In contrast to the investigated NaCl systems, a significant increase of experimental E_h is observed with increasing $MgCl_2$ concentration (Figure 4c). As occurring for Sn(II) systems, this observation indicates that the Fe(II)/Fe(III) redox couple is significantly influenced by ionic strength, $[Cl^-]$ and/or $[Mg^{2+}]$. Concentration of Tc in solution remains unaffected for samples in the acidic pH region with E_h values above the calculated Tc(VII)/Tc(IV) borderline (Figure 4d), thus indicating the predominance of Tc(VII). These observations are further confirmed by solvent extraction analysis as summarized in Table 3. The sample at $pH_c \sim 3.5$ and $E_h = 0.2$ V in 0.25 M $MgCl_2$ is the only sample in this pH region below the Tc(VII)/Tc(IV) borderline for which unexpectedly no decrease of [Tc] is observed within 395 d. In general, a very good agreement between experimental data and thermodynamic calculations is observed for $MgCl_2$ solutions under near-neutral to alkaline pH conditions ($6 \leq pH_c \leq 9$). All samples in this pH region with E_h values below the Tc(VII)/Tc(IV) borderline show a clear decrease in [Tc] and consequent reduction to Tc(IV). As in the case of Sn(II) systems, slow kinetics are observed in 4.5 M $MgCl_2$ at $pH_c = pH_{max}$, where $[Tc]_{aq}$ decreases from $\sim 10^{-7.3}$ M to $\sim 10^{-8.3}$ M within 395 d. The very low concentration of Tc reached in these conditions compared to Sn(II) systems and undersaturation solubility experiments (see Figure 3) indicate that sorption of Tc(IV) on the forming magnetite may have occurred.

4.1.4 Corroding Fe powder systems

Very reducing E_h values are measured in the presence of Fe corroding powder in diluted NaCl and $MgCl_2$ systems at $pH_c \leq 9$ (Figs. 5a and 5c). These values are in good agreement with previous studies under analogous experimental conditions at $pe + pH = 2 \pm 1$ [48]. A fast reduction of Tc(VII) to Tc(IV) is observed for all samples at $pH_c \leq 9$, as indicated by the decrease of [Tc] (Figure 5b) and confirmed by solvent extraction (Table 3). Above $pH_c \sim 10$, the reducing capacity of Fe powder is retained only for ~ 60 days. A similar behaviour of Fe powder in 0.1 M NaCl solutions was recently reported by Kobayashi *et al.* (2013) [23]. E_h

values measured after this time are situated above the Tc(VII)/Tc(IV) redox borderline, corresponding to the predominance of Tc(VII) in solution with [Tc] ~ 10^{-5} M. These results again show that reliable E_h values can be measured in Fe redox-buffered systems (also at high I). They also indicate that the NEA–TDB selection of thermodynamic data in combination with SIT/Pitzer ion interaction parameters reported in the present study (see Sect. 2) offer an accurate tool to predict Tc redox behaviour in dilute to concentrated brine solutions.

4.2 Tc reduction and sorption by Fe phases

4.2.1 Wet chemistry data

Magnetite and mackinawite synthesized in this work were positively identified by their XRD patterns (JCPDS–files 19-0629 and 24-0073) after the equilibration with the corresponding NaCl and $MgCl_2$ solutions for 2 weeks (data not shown). This confirms that no solid phase transformation took place in the concentrated brines at the given pH conditions. E_h and pH_c values measured in the Fe mineral suspensions (magnetite, mackinawite and siderite) after 4 weeks equilibration time are summarized in Table 4. In all cases, experimental E_h values are below the observed Tc(VII)/Tc(IV) reduction borderline. Analog to previous observations for other reducing systems reported in this work, E_h values in 4.5 M $MgCl_2$media are significantly higher than in 5.0 M NaCl (~ 2 pe-units) at the same pH_c, characteristic for a redox couple strongly impacted by ionic strength, [Cl^-] and/or [Mg^{2+}].

R_d values ($R_d = \frac{[Tc]_s}{[Tc]_{aq}} \cdot \frac{V}{m}$, in L kg^{-1}) were derived from experimental data to assess Tc sorption properties in saline samples (see Table 4). A stronger uptake is observed in 5.0 M NaCl ($4.6 \le \log R_d(L\,kg^{-1}) \le 7.2$) compared to sorption samples in 4.5 M $MgCl_2$ ($3.0 \le \log R_d(L\,kg^{-1}) \le$ 4.1). This is consistent with the expected shift of the sorption edge of Tc(IV) towards higher pH_c values with increasing ionic strength, similar to observations made for hydrolysis ([12], p.w.). Note that a similar effect of ionic strength on sorption was recently reported by Schnurr *et al.* for the uptake of Eu(III) by illite [49], where a much stronger decrease of sorption in the presence of divalent cations (Ca^{2+} and Mg^{2+}) was observed.

Table 4: pH_c, E_h and $\log R_d$ values determined for the uptake of Tc by Fe minerals (after 4 weeks of equilibration time).

Fe mineral	Background electrolyte	pH_c [a]	E_h (mV) [b]	$\log R_d$ (L kg^{-1}) [c]
Magnetite	5.0 M NaCl	9.6	−140	4.7
Magnetite	4.5 M $MgCl_2$	8.7	10	3.0
Mackinawite	5.0 M NaCl	8.7	−290	7.2
Mackinawite	4.5 M $MgCl_2$	8.3	−150	4.1
Siderite	5.0 M NaCl	8.7	−175	6.0
Siderite	4.5 M $MgCl_2$	8.3	−25	3.8

a: ±0.05; b: ±100 mV; c: ±10% for $\log R_d \le 3$; ±50% for $\log R_d \ge 3$.

4.2.2 XANES analysis

Figure 6 shows the X-ray absorption near-edge structure (XANES) spectra measured at the Tc K-edge, for Fe(II) minerals reacted with Tc(VII). The spectra were collected at a sample temperature of 10–15 K in He atmosphere to prevent eventual changes of Tc oxidation state by atmospheric O_2 or by O-radicals produced by the high X-ray photon flux. All mineral samples have an edge position near 21.058 keV and a white line position at 21.065 to

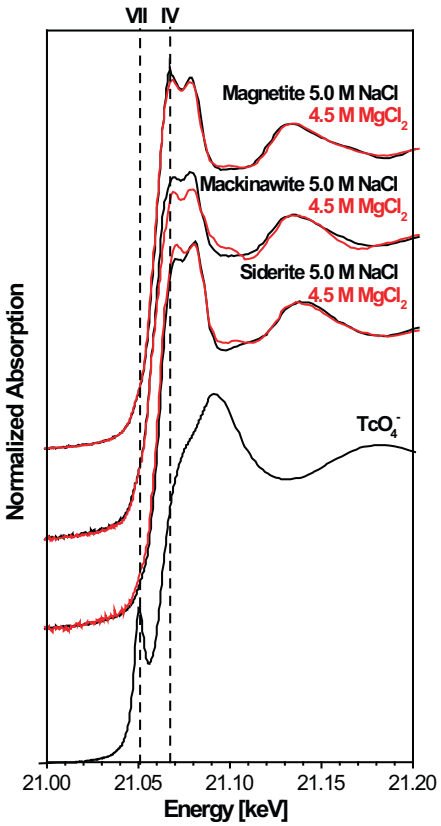

Fig. 6: Tc K-edge XANES spectra of Tc(VII) reacted with magnetite, mackinawite and siderite (see Table 4 for sample description). Bottom XANES spectrum corresponding to a TcO_4^- reference sample. The reader is referred to previous publications for the XANES spectra of a TcO_2(s) reference [20, 50, 51].

21.070 eV in line with Tc(IV), while the distinct pre-edge peak of Tc(VII) at 21.050 keV is absent in these samples. Accordingly, Tc(VII) has been reduced to Tc(IV) in all the samples. The edge and white line positions as well as the fine structure is furthermore suggesting a coordination to O atoms; therefore, we find no evidence for the (partial) coordination of Tc(IV) by S atoms in the high-salt mackinawite systems. This is in contrast to previous work, where formation of a TcS_2-like phase was found after precipitating mackinawite in the presence of pertechnetate [18, 19]. Tc(IV) coordinated to S was also found after sorption of pertechnetate to mackinawite at an ionic strength of 0.1 M [18, 19, 23], pointing to a decisive role of ionic strength on the reaction product, but this needs confirmation by more detailed investigations.

5 Conclusion

A comprehensive understanding of technetium redox processes is essential for the reliable estimation of solubility limits and technetium source term in the context of nuclear waste disposal. In the case of nuclear waste disposal in rock salt or other sites with potentially high ionic strength solutions present, a detailed understanding of Tc redox processes under these specific conditions is required.

Tc(VII)/Tc(IV) redox behaviour was systematically studied in dilute to concentrated NaCl and $MgCl_2$ solutions. In the investigated redox-buffered systems, the assessment of experimental pH and E_h values by thermodynamic calculations using NEA–TDB data provides an accurate tool to predict the redox distribution of Tc in aqueous solutions. The use of SIT and Pitzer ion interaction coefficients proposed in this work allows to extend the predictions to concentrated NaCl and $MgCl_2$ brine systems. A systematic increase of experimental E_h values is related to increasing ionic strength, especially in concentrated $MgCl_2$ brines. This observation reflects the impact of ionic strength, choride- and/or magnesium concentration on the redox couple controlling the redox potential of the solution. In redox-buffered systems where the two members of the redox couple (and corresponding thermodynamics) are known (*i.e.* Fe(II)/Fe(III) under acidic conditions), measured and thermodynamically calculated E_h values show a very good agreement.

The solubility of Tc(IV) in concentrated $MgCl_2$ solutions (2.0 M and 4.5 M) is significantly enhanced compared with diluted NaCl and $MgCl_2$ systems. This can be explained by the stabilization of charged hydrolysis species at elevated ionic strengths, although the formation of new Tc(IV) aqueous species (*i.e.* Tc(IV)–OH–Cl or Mg–Tc(IV)–OH) cannot be ruled out.

Tc(VII) is reduced and strongly sorbed ($\log R_d \geq 3\ L\ kg^{-1}$) by magnetite, mackinawite and siderite under mildly alkaline conditions in concentrated NaCl and $MgCl_2$ solutions. Analog to the behaviour observed in homogeneous systems, Tc(IV) is stabilized in the aqueous phase in concentrated $MgCl_2$ solutions resulting in a weaker sorption compared to dilute systems or concentrated NaCl solutions. To our knowledge, this is the first experimental study providing quantitative data on the uptake of Tc by corrosion products of Fe in concentrated brine solutions.

Appendix

Table A1: Thermodynamic data for Fe(II)/Fe(III) used to calculate Fe systems under acidic conditions.

Reaction	$\log {}^*K^\circ$	Reference
$Fe^{2+} \Leftrightarrow Fe^{3+} + e^-$	−13.05	NEA-TDB [52]
$Fe^{3+} + Cl^- \Leftrightarrow FeCl^{2+}$	1.52	NEA-TDB [52]
$Fe^{3+} + 2Cl^- \Leftrightarrow FeCl_2{}^+$	2.22	NEA-TDB [52]
$Fe^{3+} + H_2O \Leftrightarrow Fe(OH)^{2+} + H^+$	−2.15	NEA-TDB [52]

Table A2: SIT ion interaction coefficients for Fe species in NaCl solutions.

i	j	ε_{ij} (mol kg^{-1})	References
H^+	Cl^-	0.12	NEA-TDB [24]
OH^-	Na	0.04	NEA-TDB [24]
Fe^{3+}	Cl^-	0.24	estimated from $\varepsilon(Fe^{3+}, ClO_4{}^-) = 0.56$[a]
Fe^{2+}	Cl^-	0.16	estimated from $\varepsilon(Fe^{2+}, ClO_4{}^-) = 0.38$[a]
$FeCl^{2+}$	Cl^-	0.15	estimated by charge correlation[b]
$FeCl_2{}^+$	Cl^-	0.05	estimated by charge correlation[b]
$FeOH^{2+}$	Cl^-	0.15	estimated by charge correlation[b]

a: The SIT coefficients for the interaction with Cl^- are estimated from the corresponding SIT coefficients for the interaction with $ClO_4{}^-$ [24] according with the correlation: $\varepsilon(M^{z+}, Cl^-) = 0.38\ \varepsilon(M^{z+}, ClO_4{}^-) \pm 0.02$ mol kg^{-1} [53];
b: [54].

Acknowledgement: This work was partially supported by the German Federal Ministry of Economics and Technology (BMWi) under the project of VESPA. The staff of the ROBL beamline at ESRF and Dr. M. Marques Fernandes (PSI–LES, Switzerland) are kindly acknowledged for the assistance during EXAFS measurements. Thanks are extended to M. Böttle and Dr. D. Fellhauer (KIT–INE) for sup-

port in the preparation of the Fe phases and Pitzer calculations.

References

1. Blanchard, D. L., Brown, G. N., Conradson, S. D., Fadeff, S. K., Golcar, G. R., Hess, N. J., Klinger, G. S., Kurath, D. E.: Technetium in alkaline, high-salt radioactive tank waste supernate: preliminary chracterization and removal, PNNL-11386 UC-2030 (1997).
2. Kupfer, M. J., Boldt, A. L., Hodgson, K. M., Shelton, L. W., Simpson, B. C., Watrous, R. A., Leclaire, M. D., Borsheim, G. L., Winward, R. T., Higley, B. A., Orme, R. M., Colton, N. G., Lambert, S. L., Place, D. E., Schulz, W. W.: Standart inventories of chemicals and radionuclides in Hanford site tank wastes, HNF-SD-WM-740 (1999).
3. Altmaier, M., Neck, V., Lützenkirchen, J., Fanghänel, T.: Solubility of plutonium in $MgCl_2$ and $CaCl_2$ solutions in contact with metallic iron. Radiochim. Acta **97**, 187–192 (2009).
4. Neck, V., Altmaier, M., Rabung, T., Lützenkirchen, J., Fanghänel, T.: Thermodynamics of trivalent actinides and neodymium in NaCl, $MgCl_2$, and $CaCl_2$ solutions: Solubility, hydrolysis, and ternary Ca-M(III)-OH complexes. Pure Appl. Chem. **81**, 1555–1568 (2009).
5. Fellhauer, D., Neck, V., Altmaier, M., Lützenkirchen, J., Fanghänel, T.: Solubility of tetravalent actinides in alkaline $CaCl_2$ solutions and formation of $Ca_4[An(OH)_8]^{4+}$ complexes: a study of Np(IV) and Pu(IV) under reducing conditions and the systematic trend in the An(IV) series. Radiochim. Acta **98**, 541–548 (2010).
6. Russell, C. D., Cash, A.: Products of pertechnetate reduction in complexing media. J. Nucl. Med. **19**, 694–694 (1978).
7. Grassi, J., Rogelet, P., Devynck, J., Tremillon, B.: Radiopolarography of technetium(VII) in acidic medium. J. Electroanal. Chem. **88**, 97–103 (1978).
8. Grassi, J., Devynck, J., Tremillon, B.: Electrochemical studies of technetium at a mercury-electrode. Anal. Chimica Acta **107**, 47–58 (1979).
9. Poineau, F., Fattahi, M., Den Auwer, C., Hennig, C., Grambow, B.: Speciation of technetium and rhenium complexes by in situ XAS-electrochemistry. Radiochim. Acta **94**, 283–289 (2006).
10. Owunwanne, A., Marinsky, J., Blau, M.: Charge and nature of technetium species produced in reduction of pertechnetate by stannous ion. J. Nucl. Med. **18**, 1099–1105 (1977).
11. Warwick, P., Aldridge, S., Evans, N., Vines, S.: The solubility of technetium(IV) at high pH. Radiochim. Acta **95**, 709–716 (2007).
12. Hess, N. J., Xia, Y. X., Rai, D., Conradson, S. D.: Thermodynamic model for the solubility of $TcO_2 \cdot xH_2O(am)$ in the aqueous $Tc(IV)$-Na^+-Cl^--H^+-OH^--H_2O system. J. Solut. Chem. **33**, 199–226 (2004).
13. Cui, D. Q., Eriksen, T. E.: Reduction of pertechnetate by ferrous iron in solution: Influence of sorbed and precipitated Fe(II). Environ. Sci. Technol. **30**, 2259–2262 (1996).
14. Zachara, J. M., Heald, S. M., Jeon, B. H., Kukkadapu, R. K., Liu, C. X., McKinley, J. P., Dohnalkova, A. C., Moore, D. A.: Reduction of pertechnetate [Tc(VII)] by aqueous Fe(II) and the nature of solid phase redox products. Geochim. Cosmochim. Acta **71**, 2137–2157 (2007).
15. Cui, D. Q., Eriksen, T. E.: Reduction of pertechnetate in solution by heterogeneous electron transfer from Fe(II)-containing geological material. Environ. Sci. Technol. **30**, 2263–2269 (1996).
16. Geraedts, K., Bruggeman, C., Maes, A., Van Loon, L. R., Rossberg, A., Reich, T.: Evidence for the existence of Tc(IV)-humic substance species by X-ray absorption near-edge spectroscopy. Radiochim. Acta **90**, 879–884 (2002).
17. Maes, A., Geraedts, K., Bruggeman, C., Vancluysen, J., Rossberg, A., Hennig, C.: Evidence for the interaction of technetium colloids with humic substances by X-ray absorption spectroscopy. Environ. Sci. Technol. **38**, 2044–2051 (2004).
18. Wharton, M. J., Atkins, B., Charnock, J. M., Livens, F. R., Pattrick, R. A. D., Collison, D.: An X-ray absorption spectroscopy study of the coprecipitation of Tc and Re with mackinawite (FeS). Appl. Geochem. **15**, 347–354 (2000).
19. Livens, F. R., Jones, M. J., Hynes, A. J., Charnock, J. M., Mosselmans, J. F. W., Hennig, C., Steele, H., Collison, D., Vaughan, D. J., Pattrick, R. A. D., Reed, W. A., Moyes, L. N.: X-ray absorption spectroscopy studies of reactions of technetium, uranium and neptunium with mackinawite. J. Environ. Radioact. **74**, 211–219 (2004).
20. Liu, Y., Terry, J., Jurisson, S.: Pertechnetate immobilization with amorphous iron sulfide. Radiochim. Acta **96**, 823–833 (2008).
21. Llorens, I. A., Deniard, P., Gautron, E., Olicard, A., Fattahi, M., Jobic, S., Grambow, B.: Structural investigation of coprecipitation of technetium-99 with iron phases. Radiochim. Acta **96**, 569–574 (2008).
22. Peretyazhko, T. S., Zachara, J. M., Kukkadapu, R. K., Heald, S. M., Kutnyakov, I. V., Resch, C. T., Arey, B. W., Wang, C. M., Kovarik, L., Phillips, J. L., Moore, D. A.: Pertechnetate (TcO_4^-) reduction by reactive ferrous iron forms in naturally anoxic, redox transition zone sediments from the Hanford Site, USA. Geochim. Cosmochim. Acta **92**, 48–66 (2012).
23. Kobayashi, T., Scheinost, A. C., Fellhauer, D., Gaona, X., Altmaier, M.: Redox behavior of $Tc(VII)/Tc(IV)$ under various reducing conditions in $0.1\ M$ NaCl solutions. Radiochim. Acta **101**, 323–332 (2013).
24. Guillaumont, R., Fanghänel, T., Neck, V., Fuger, J., Palmer, D. A., Grenthe, I., Rand, M. H.: *Update on the Chemical Thermodynamics of Uranium, Neptunium, Plutonium, Americium and Technetium*. OECD Nuclear Energy Agency (ed.), Vol. 5, North-Holland, Amsterdam, Elsevier (2003).
25. Rard, J. A., Rand, M. H., Anderegg, G., Wanner, H.: *Chemical Thermodynamics of Technetium*. (Sandino, M. C. A., Östhols, E., eds.) Vol. 3, North-Holland, Amsterdam, Elsevier (1999).
26. Chotkowski, M., Czerwinski, A.: Electrochemical and spectroelectrochemical studies of pertechnetate electroreduction in acidic media. Electrochim. Acta **76**, 165–173 (2012).
27. Ciavatta, L.: The specific interaction theory in equilibrium-analysis – some empirical rules for estimating interaction coefficients of metal-ion complexes. Ann. Chim. **80**, 255–263 (1990).
28. Grenthe, I., Wanner, H., Östhols, M.: Guidelines for the Extrapolation to Zero Ionic Strength. Nuclear Energy Agency, OECD (2000).
29. Pitzer, K. S.: *Activity Coefficients in Electrolyte Solutions*. Chap. 3, Boca Raton, FL (1991).

30. Harvie, C. E., Moller, N., Weare, J. H.: The prediction of mineral solubilities in natural-waters – the Na-K-Mg-Ca-H-Cl-SO_4-OH-HCO_3-CO_3-CO_2-H_2O system to high ionic strengths at 25 °C. Geochim. Cosmochim. Acta **48**, 723–751 (1984).
31. Konnecke, T., Neck, V., Fanghänel, T., Kim, J. I.: Activity coefficients and Pitzer parameters in the systems $Na^+/Cs^+/Cl^-/TcO_4^-$ or ClO_4^-/H_2O at 25 °C. J. Solut. Chem. **26**, 561–577 (1997).
32. Neck, V., Konnecke, T., Fanghänel, T., Kim, J. I.: Pitzer parameters for the pertechnetate ion in the system $Na^+/K^+/Mg^{2+}/Ca^{2+}/Cl^-/SO_4^{2-}/TcO_4^-/H_2O$ at 25 °C. J. Solut. Chem. **27**, 107–120 (1998).
33. Kirsch, R., Fellhauer, D., Altmaier, M., Neck, V., Rossberg, A., Fanghänel, T., Charlet, L., Scheinost, A. C.: Oxidation state and local structure of plutonium reacted with magnetite, mackinawite and chukanovite. Environ. Sci. Technol. **45**, 7267–7274 (2011).
34. Altmaier, M., Metz, V., Neck, V., Muller, R., Fanghänel, T.: Solid-liquid equilibria of $Mg(OH)_2(cr)$ and $Mg_2(OH)_3Cl \cdot 4H_2O(cr)$ in the system Mg-Na-H-OH-O-Cl-H_2O at 25 °C. Geochim. Cosmochim. Acta **67**, 3595–3601 (2003).
35. Bischofer, B. P., Hagemann, S., Hühne, C., Schönwiese, D., Scharge, T.: Influence of chloride concentrations on the signal of redox electrode and on UV-spectrophotometric determination of Fe species. In 1st Annual Workshop Proceedings *7th* EC FP-Recosy CP, Barcelona (2009).
36. Scharge, T., Bischofer, B. P., Hagemann, S., Schönwiese, D.: Spectrophotometric and potentiometric determination of the redox potential in solutions of high ionic strength. In: 2nd Annual Workshop Proceeding 7th EC FP-Recosy CP, Cyprus (2010).
37. Barry, P. H.: JPCALC, a software package for calculating liquid-junction potential corrections in patch-clamp, intracellular, epithelial and bilayer measurements and for correcting junction potential measurements. J. Neurosci. Methods **51**, 107–116 (1994).
38. Omori, T., Muraoka, Y., Suganuma, H.: Solvent-extraction mechanism of pertechnetate with tetraphenylarsonium chloride. J. Radioanal. Nucl. Chem.-Art. **178**, 237–243 (1994).
39. Kopunec, R., Abudeab, F. N., Skraskova, S.: Extraction of pertechnetate with tetraphenylphosphonium in the presence of various acids, salts and hydroxides. J. Radioanal. Nucl. Chem. **230**, 51–60 (1998).
40. Gaona, X., Dähn, R., Tits, J., Scheinost, A. C., Wieland, E.: Uptake of Np(IV) by C-S-H phases and cement paste: an EXAFS study. Environ. Sci. Technol. **45**, 8765–8771 (2011).
41. Saeki, M., Sasaki, Y., Nakai, A., Ohashi, A., Banerjee, D., Scheinost, A. C., Foerstendorf, H.: Structural study on 2,2′-(methylimino)bis(*N*,*N*-dioctylacetamide) complex with $Re(VII)O_4^-$ and $Tc(VII)O_4^-$ by ^1H NMR, EXAFS, and IR spectroscopy. Inorg. Chem. **51**, 5814–5821 (2012).
42. Meyer, R. E., Arnold, W. D.: The electrode potential of the Tc(IV)-Tc(VII) couple. Radiochim. Acta **55**, 19–22 (1991).
43. Lem, W. J., Wayman, M.: Decomposition of aqueous dithionite. 1. Kinetics of decomposition of aqueous sodium dithionite. Can. J. Chem. **48**, 776 (1970).
44. Wayman, M., Lem, W. J.: Decomposition of aqueous dithionite. 2. A reaction mechanism for decomposition of aqueous sodium dithionite. Can. J. Chem. **48**, 782 (1970).
45. Stern, H. S., Mcafee, J. G., Subraman, G.: Preparation distribution and utilization of technetium-99m-sulfur colloid. J. Nucl. Med. **7**, 665 (1966).
46. Eriksen, T. E., Ndalamba, P., Bruno, J., Caceci, M.: The solubility of $TcO_2 \cdot nH_2O$ in neutral to alkaline-solutions under constant p_{CO_2}. Radiochim. Acta **58–59**, 67–70 (1992).
47. Morrison, G. H., Freiser, H.: *Solvent Extraction in Analytical Chemistry*. John Willey & Sons, Inc., London (1957).
48. Felmy, A. R., Rai, D., Schramke, J. A., Ryan, J. L.: The solubility of plutonium hydroxide in dilute-solution and in high-ionic-strength chloride brines. Radiochim. Acta **48**, 29–35 (1989).
49. Schnurr, A., Marsac, R., Rabung, T., Lützenkirchen, J., Geckeis, H.: Investigation of actinide and lanthanide sorption on clay minerals under saline conditions, in: Migration Conference, Brighton, United Kingdom (2013).
50. Liu, Y., Terry, J., Jurisson, S.: Pertechnetate immobilization in aqueous media with hydrogen sulfide under anaerobic and aerobic environments. Radiochim. Acta **95**, 717–725 (2007).
51. Um, W., Chang, H. S., Icenhower, J. P., Lukens, W. W., Serne, R. J., Qafoku, N. P., Westsik, J. H., Buck, E. C., Smith, S. C.: Immobilization of 99-technetium(VII) by Fe(II)-goethite and limited reoxidation. Environ. Sci. Technol. **45**, 4904–4913 (2011).
52. Lemire, R. J., Berner, U., Musikas, C., Palmer, D. A., Taylor, P., Tochiyama, O.: Chemical thermodynamics of iron, ed. OECD Nuclear Energy Agency. Vol. 13a. Issy-les-Moulineaux, France (2013).
53. Neck, V., Altmaier, M., Fanghänel, T.: Ion interaction (SIT) coefficients for the Th^{4+} ion and trace activity coefficients in $NaClO_4$, $NaNO_3$ and NaCl solution determined by solvent extraction with TBP. Radiochim. Acta **94**, 501–507 (2006).
54. Hummel, W.: Ionic strength corrections and estimation of SIT ion interaction coefficients, PSI report, TM-44-09-01, Paul Scherrer Institut, Villigen (Switzerland) (2009).